Journal of Electronic Materials (2024) 53:1142–1160
https://doi.org/10.1007/s11664-023-10852-6

ORIGINAL RESEARCH ARTICLE

Incomplete Ionization-Dependent Carrier Mobility in Silicon-on-Insulator *n-p-n* Double-Gate Tunnel Field-Effect Transistors

Priyam Pathak[1] · Deepjyoti Deb[1] · Dwipayan Nath[1] · Prachuryya Subash Das[1] · Hirakjyoti Choudhury[1] · Rupam Goswami[1]

Received: 21 March 2023 / Accepted: 21 November 2023 / Published online: 16 January 2024
© The Minerals, Metals & Materials Society 2024

Abstract

This article reports the effects of incomplete ionization on the low power performance of silicon-on-insulator (SOI) *n-p-n* dual-gate tunnel field-effect transistors (TFET) through calibrated technology computer-aided design simulations. The effects of drain-induced barrier thinning and resistivity profiles are reported for the proposed device in the presence and absence of incomplete ionization. A current sensitivity parameter is considered for analysis, which refers to the deviation of the drain current of the device with incomplete ionization included from the case without incomplete ionization. Considering the Altermatt incomplete ionization parameters for boron and arsenic dopants in the device of interest, this article presents the investigation of incomplete ionization for various gate work functions, and mobility models (doping-dependent models: Masetti, Arora, and Philips Unified, and mobility degradation models: University of Bologna, Lombardi, and Inversion and Accumulation Layer). The impact of a trap-assisted tunneling model on sensitivity is also reported.

Keywords Incomplete ionization · *n-p-n* TFET · critical doping · doping-dependent mobility · mobility degradation

Introduction

Due to its ability to have a sub-threshold swing value of less than 60mV/decade, tunnel field-effect transistors (TFET) are one of the most promising choices among the several alternatives to metal–oxide–semiconductor field–effect transistors (MOSFET) for future very large-scale industry applications.[1,2] Tunnel field effect transistors (TFETs) use in low-power and high-speed activities hampers the thermal limit of the MOSFET subthreshold swing, which prevents the threshold voltage from being lowered. A TFET is a superior choice for high-speed operations with little OFF current dissipation because it is not constrained by this thermal tail.[3] The working concept of this transistor, which has a fundamental structure of a gated PIN diode, is bias-controlled band-to-band tunneling (BTBT).[4] Generally, charge carriers tunnel via the potential barrier between the source valence band and the channel conduction band to cause current creation in TFETs. Lower energy is associated with its operation, making a MOSFET a viable low-power device.[2] This is because we are using electrons in their lower energy or more stable state rather than the state formed by thermionic emissions in the case of the MOSFET, which is more randomly distributed and unstable. Compared to a MOSFET, a TFET provides a number of benefits, including improved resistance to short channel effects and a larger I_{ON}/I_{OFF} current ratio.[1,2]

Due to these characteristics, TFETs are grabbing lots of attention from the research fraternity. However, a few demerits still prevail which is hampering its widespread use in VLSI circuit implementation, including ambipolar current and low ON current.[5,6] In this paper, we are formulating a methodology to potentially enhance the ON current of the device using a naturally occurring phenomenon associated with dopants in semiconductors called incomplete ionization. Incomplete ionization, which we generally associate with a current degrading phenomenon can be potentially used to enhance the ON current of the device by its proper utilization across the source region of the TFET, filling the valence band with more electrons, hence increasing the

✉ Rupam Goswami
rupam21@tezu.ernet.in

[1] Technology in Semiconductors and Devices Laboratory, Department of Electronics and Communication Engineering, Tezpur University, Napaam, Assam 784028, India

tunneling current probability. We observe the effects of incomplete ionization for various mobility models and at the same time propose a concept to enhance the ON current of the TFET by varying the N_{crit} values.[7]

Incomplete ionization is a phenomenon observed in semiconductors in which the dopant species are not completely utilized for their contribution of free carriers. Under this condition, a few donor atoms remain unionized in the donor energy level and a fraction of the electrons does not reach the conduction band. Similarly, a few acceptor atoms are devoid of electrons from the valence band (meaning holes from the acceptor energy level to the valence band) leading to incomplete ionization of the acceptor atoms. Although incomplete ionization is highly influential for silicon devices at low temperatures, yet it is observed that there is a considerable amount of incomplete ionization at room temperature. For dopants like arsenic, boron, and phosphorous with low dopant concentrations, there is a discrete dopant energy level E_{Dop} situated below (above) the conduction band (valence band). The discrete dopant energy levels form an energy band because of clusters of dopants formed in silicon due to moderate doping concentrations.[8] Increasing the doping concentration increases the cluster size which again increases the probability of the movement of electrons from one cluster to another, thereby increasing the electron concentration of the conduction band.[9]

At considerably higher doping concentrations, where the concentration reaches a critical value, N_{crit}, the dopant band touches the conduction band or the valence band, leading to a change in the behavior of conduction identified by a phenomenon known as the Mott metal–insulator (M-I) transition.[8] An impurity band enters the majority carrier concentration band for maximum doping and hence the idea of a separate band is trivial.[10] Here, the Fermi–Dirac distribution along with the dopant impurities are mentioned in Eqs. 1 and 2[11]:

$$N_{\mathrm{D}} = \frac{N_{\mathrm{D0}}}{1 + g_D.\exp(\frac{E_{\mathrm{FN}} - E_{\mathrm{D}}}{\mathrm{KT}})} \quad (1)$$

$$N_{\mathrm{A}} = \frac{N_{\mathrm{A0}}}{1 + g_A.\exp(\frac{E_{\mathrm{A}} - E_{\mathrm{FP}}}{\mathrm{KT}})} \quad (2)$$

where E_{FN} (E_{FP}) is the quasi-Fermi energy level for electrons (holes), g_{D} (g_{A}) is the degeneracy factor for donors (acceptors), and $E_{\mathrm{D}}(E_{\mathrm{A}})$ is the donor and acceptor level. Despite the fact that B -doped silicon has a smaller lower ionization energy than P-doped silicon ($E_{\mathrm{B},0} = 44.4\mathrm{meV} \mathrm{vs.} E_{P,0} = 45.5\mathrm{meV}$), incomplete ionization is predicted to be stronger in B -doped silicon than in P -doped silicon. There are two degenerate valence bands for acceptors which is why they are fourfold degenerate, whereas donors are only twofold degenerate, allowing each donor level to accept one electron of either spin. This is because acceptors have two degenerate valence bands and donors only have one degenerate level, allowing each donor level to accept one hole of either spin.[12] N_{D} (N_{A}) is the activated number of donors (acceptors), N_{D0} and N_{A0} is the total donor (acceptor) concentration, E_{D} (E_{A}) is the energy level for donors (acceptor), T is the absolute temperature in Kelvin, and $K$is the Boltzmann constant. Corresponding values of N_{crit} due to different doping species lead to different degrees that are available for the carriers to conduct.

Incomplete ionization can be significant in unconventional transistors like TFETs. The quantum mechanical BTBT current in TFETs is not merely dependent on the parameters of the tunnel barrier but also on the availability of carriers at the source end of the barrier, which is interpreted by the Fermi–Dirac distribution in the source region. Investigation of incomplete ionization in TFETs has not yet been reported.

With this objective, this article reports the impact of incomplete ionization on the performance of *n-p-n* SOI double-gate TFETs with arsenic and boron acting as doping species in the drain and source regions of the transistor, respectively. Since this investigation is carried out for the first time, different mobility models are considered for evaluating the impact of incomplete ionization on the device performance. This work further aims to offer information on the response of the mobility models towards the phenomenon of incomplete ionization as different mobility models under ideal and non-ideal conditions may be potentially used for computational purposes, which include validation of experimental data, calibration of mobility models in TFETs, and the design of analytical models for circuit simulations. Therefore, the investigation carried out in this work has a wider scope and contributes significantly to the unexplored domain of incomplete ionization in TFETs.

Section "Architecture and Simulation Set-up" shows the architecture and simulation set-up of the device while Sect. "Significance Of Incomplete Ionization" presents the importance of incomplete ionization. Section "Results and Discussion" presents the results associated with the investigation. Section "Conclusions" summarizes and concludes the article.

Architecture and Simulation Set-up

The double-gate *n-p-n* TFET considered in this work is shown in Fig. 1, in which the *p*-type region acting as the source is sandwiched between two *n*-type regions acting as drains. The device has dual gates present across the two

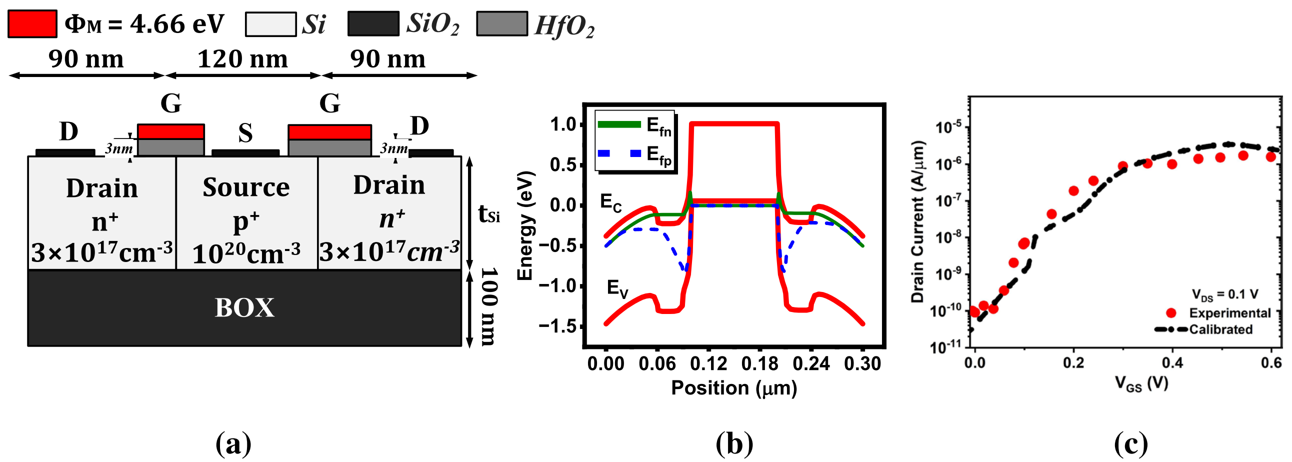

Doping Dependence Mobility Models

Philips Unified Models

Masetti Models

Arora Models

Mobility Degradation Models

University of Bologna Model

Lombardi Model

Inversion Accumulation Layer Model

(d)

Fig. 1 (a) 2-D architecture of proposed device; (b) energy band diagram at $V_{GS} = 1V$, $V_{DS} = 0.5V$; (c) calibration curve[13]; (d) flow chart of the calibrated and theoretical mobility models.

junctions, while HfO_2 material is used as the gate oxide of the device having a thickness (t_{ox}) of 3nm. The drain regions each 90nm long are doped with an arsenic concentration of $3 \times 10^{17} cm^{-3}$. *The source is* 120nm *long and* doped with a boron concentration of $10^{20} cm^{-3}$. The thickness of the silicon (t_{Si}) is 10nm, while the buried oxide has a thickness of 100nm.[14] These device dimensions are used for all the simulations, keeping the drain source voltage (V_{DS}) and work function (φ_M) constant at 0.5V and 4.2eV, respectively, unless otherwise specified.

Simulations have been carried out using the Sentaurus TCAD tool.[15] A Schenk BTBT model has been implemented in the simulations. An incomplete ionization model has been included in the simulations to take into consideration the effect of incomplete ionization for the said dopants in the device. Band gap narrowing, doping-dependent mobility models, and Fermi–Dirac statistics are implemented due to the high doping concentration in the device.

Three doping-dependent mobility models are considered in this work. Among them, the Masetti and Arora mobility models are fundamental doping-dependent mobility models.[16,17] Similarly, the Philips Unified mobility model is also implemented in the simulations to take into account the effects of the clustering of the dopants.[18] The interface mobility degradation model's effect has also been taken into consideration, which includes the University of Bologna, Lombardi, and inversion and accumulation layer (IAL) mobility models.[18,20,21] For acoustic phonon scattering and surface roughness scattering, the Lombardi model comes into the picture.[19] The IAL mobility model comprises transverse field and doping dependencies which contains 2-D Coulomb impurity scattering. For the University of Bologna mobility degradation model, the decreasing factor of Coulomb scattering at low fields, and surface phonons and surface roughness scattering at large fields are considered.[18]

The tunneling model in the simulations has been calibrated with the experimental data in Ref. 13 , resulting in the model parameters: $A = 7 \times 10^{21} cm^{-1} s^{-1} V^{-2}, B = 1.25 \times 10^7 eV^{1.5} Vcm^{-1}$ and $\hbar\omega = 18.6 meV$. The Altermatt ionization model in the parameter file of the simulator for boron and arsenic doping concentrations was activated to take into consideration the specific effects of the arsenic and boron dopants in terms of ionization.[7–15] In order to show the gaps between the theoretical and experimental mobility, the electron mobility for the *n-p-n* device with calibrated parameters is compared in Fig. 1d with the electron mobility for the *n-p-n* device without calibrated parameters. Since the calibration framework justifies the use of parameters tuned with experimental work, we have therefore considered the electron mobility in the calibrated *n-p-n* TFET to be analogous to the experimental values, and the one with default parameters of silicon to be theoretical in nature. A current sensitivity parameter is defined as $S_{ii} = \left|\left(I_{noii} - I_{ii}\right)/I_{noii}\right|$, where I_{noii} is the drain current in the case of complete ionization of the dopants (no incomplete ionization), and I_{ii} is the drain current in the case of incomplete ionization of dopants in the double-gate *n-p-n* TFET.

Significance of Incomplete Ionization

To consider the significance of incomplete ionization in double-gate *n-p-n* TFETs, we have considered a theoretical experiment. The N_{crit} values of both acceptor (boron) and donor (arsenic) specimens were varied to further conceptualize the effect of incomplete ionization in TFETs. The dopant species will be completely ionized or be free to conduct once its doping concentration is higher than the N_{crit} value.[9] In the proposed device, the source is doped with boron implants of 10^{20} cm^{-3} , while both the drain regions are doped with arsenic implants of 3×10^{17} cm^{-3}. For the N_{crit} value of 5×10^{19} cm^{-3} , we observed a reduction of the ON current.

This is an expected outcome, as the number of free carriers across the drain regions decreases due to the effect of incomplete ionization for the arsenic dopants while the source boron dopant is still completely ionized, as the N_{crit} value is below the source doping level (Fig. 2a and b). When the N_{crit} value was considered to be 5×10^{20} cm^{-3} for both the acceptor and dopant implants, we observed an increase in the ON current of the device. This is quite opposite to our intuition of incomplete ionization, as lower ionized carriers should imply a smaller current. It was observed that the increase in the ON current for the N_{crit} value of 5×10^{20} cm^{-3} is due to the fact that more electron density is present in the valence band of the source region as there is lower hole density present in the valence band, as the boron dopants are not completely ionized. This phenomenon of incomplete ionization occurring across the source region will not allow a few valence band electrons to reside across the boron dopant level across the source region, which will in turn increase the number of tunneling electrons from the source to the drain region, increasing the current compared to a previous lower N_{crit} value of 5×10^{19} cm^{-3} (Fig. 3a and b). Apart from known modifications that can be implemented for achieving a higher ON current in TFETs, such as the use of high-permittivity (high-κ) gate dielectric, a minimized channel thickness showing one-dimensional electronic transport behavior, and an abrupt doping profile,[22] incomplete ionization can be the next potential phenomenon to boost the ON current of the device.

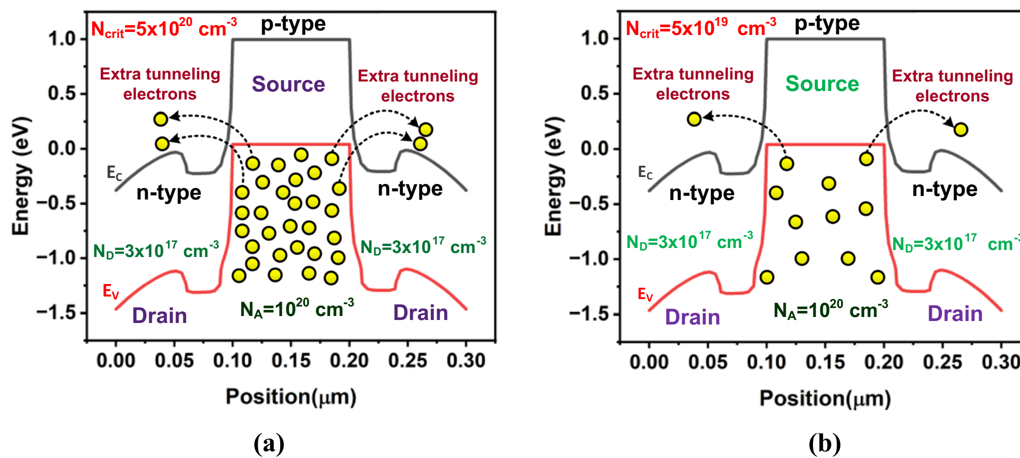

Fig. 2 An energy band diagram-based illustration of the effect of incomplete ionization on the TFET for (a) $N_{\text{crit}} = 5 \times 10^{20}\text{cm}^{-3}$, and (b)$N_{\text{crit}} = 5 \times 10^{19}\text{cm}^{-3}$.

The effect of temperature on the ionization level of donor and acceptor concentrations has been shown for the Masetti model in Fig. 3c. Since our considered N_{Critical} value of acceptor (boron) concentration is lower than the doping concentration, there is no incomplete ionization. The acceptors will be completely ionized for our case, so we have carried out a more comprehensive analysis of the ionization degree of the donor concentration with respect to temperature. With an increase in temperature across the drain region, the ionization degree of donor concentration increases. This is because the donor electrons get more energy with increasing temperature which results in getting excited in the conduction band. More donor-donated electrons are present in the conduction band, which results in a higher concentration of ionized donor concentration.

Also, in Fig. 3d, we have considered the resistivity by the equation $\rho = \frac{1}{q(\mu_e n + \mu_p p)}$ where μ_e and μ_p denotes electron and hole mobility, respectively, and n and p denote electron and hole concentrations, respectively, while q is the electronic charge. There is virtually no carrier concentration across the depletion regions, thereby enhancing the resistivity of the regions. Across the depletion regions, there is a comparatively higher resistivity for the *n-p-n* TFET suffering incomplete ionization.

High doping concentrations lead to a reduced depletion width, so the overall resistivity for high doping across the depletion region decreases. For the case with incomplete ionization, due to very limited presence of carriers, the effective doping concentration can be assumed to be reduced, which increases the depletion widths across the junctions, resulting in higher resistivity. However, across the regions, 0.20–0.25 μm and 0.05–0.08 μm, the resistivity decreases for the case with incomplete ionization. This is attributed to the high mobility associated with incomplete ionization across these regions. As we move towards the drain regions, the resistivity in the case of incomplete ionization is high compared to the ideal case of complete ionization, as the former case has a lower carrier concentration.

To verify the impact of drain-induced barrier thinning on the device, the minimum tunnel barrier width has been plotted versus the drain-to-source voltage, V_{DS} , as shown in Fig. 3e. Over the range of V_{DS}, it is observed that the tunnel barrier width is lower for the case with complete ionization compared to the case with incomplete ionization. In the former, the band bending is steeper than in the latter, which is supported by the greater availability of mobile carriers than in the latter.

Results and Discussion

In Fig. 4a, we observe the ionized acceptor concentration for the double-gate *n-p-n* TFET in the presence and absence of incomplete ionization. There is no variation of the acceptor concentration of boron across the source region as the doping concentration is above the N_{crit} ($4.06 \times 10^{18}\text{cm}^{-3}$) value. This implies that the boron dopant band has reached beyond the M-I transition which in turn make all the dopants free to conduct.[7]

In Fig. 4b, we observe the ionized donor concentration for a double-gate *n-p-n* TFET. In case of the donor arsenic dopant concentration across the drain regions, we observe a considerable amount of incompletely ionized donors as the doping concentration is below the N_{crit} ($8.5 \times 10^{18}\text{cm}^{-3}$) value.[7] We can observe the variation of donor concentration across the drain region having the highest ionized concentration close to the source and drain junction region and

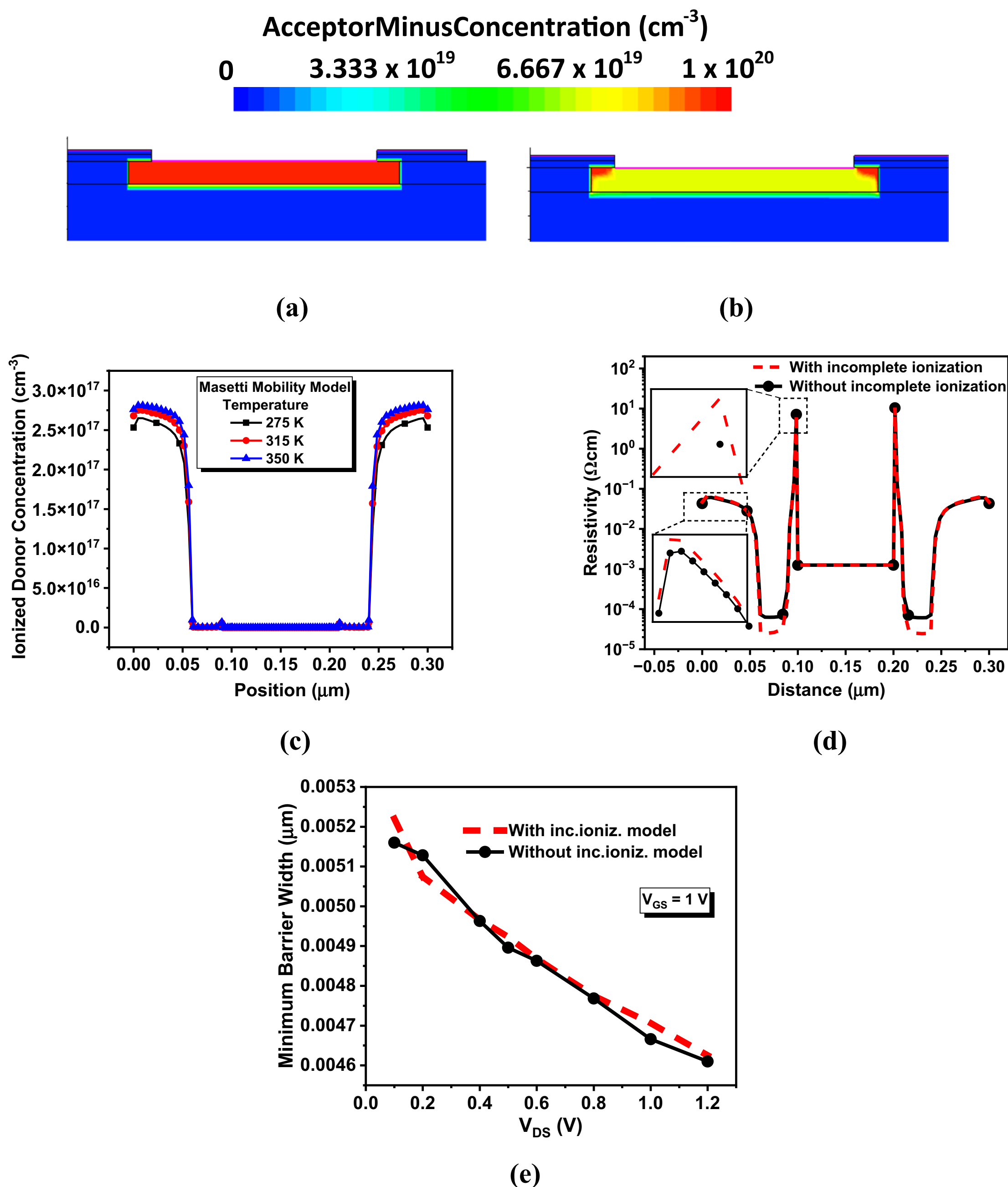

Fig. 3 (a) For $N_{crit} = 5 \times 10^{19} cm^{-3}$; (b) for $N_{crit} = 5 \times 10^{20} cm^{-3}$; (c) ionized donor concentration for different temperatures; (d) resistivity of the materials due to the incomplete ionization; (e) drain-induced barrier thinning for the proposed device.

the minimum across the gate overlapped region. The donor concentration analysis has been carried out for only one gate region as the device is symmetric in nature.

Figure 5a shows the BTBT rate for $\varphi_M = 4.05\text{eV}, 4.75\text{eV}$, whereas Fig. 5b shows the current sensitivity for various gate work functions,φ_M, plotted versus the gate-to-source voltage (V_{GS}). The sensitivity spikes move towards a positive V_{GS} regime when φ_M increases from 4.05eV to 4.66eV. Two significant observations are deduced from the plots: one, the values of the maximum sensitivity decreases, and two, the area under the curves (relative to the sensitivity spikes) in the negative V_{GS} regime increases with the increase in the gate work function. For the values of φ_M of 4.66eV and 4.75eV, a considerably higher sensitivity variation is observed across the negative V_{GS} regime.

In order to reveal the impact of gate work functions on the device under incomplete ionization, the ionized donor concentration (DonorPlusConcentration parameter in TCAD)

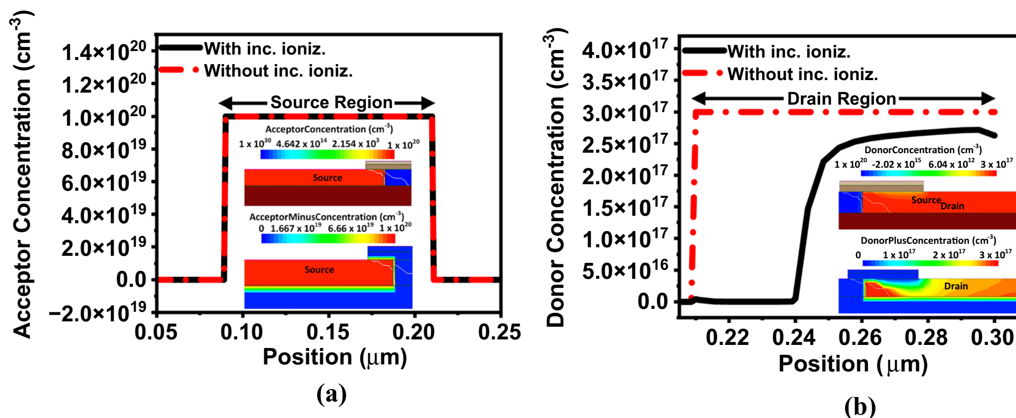

Fig. 4 (a) Ionized acceptor concentration for a double-gate *n-p-n* TFET; (b) ionized donor concentration for a double-gate *n-p-n* TFET.

and the electron density (eDensity) have been extracted at different work functions, as shown in Fig. 5c. The n^+ drain has been predominantly taken as the region of observation because the dopants in the source region are completely ionized. The ionized donor concentration increases with increasing work function. This is due to the fact that the electron carrier concentration decreases with increasing work function. The donor plus concentration here is a localized concept, which depends on the value of the Fermi level as evident from Eq. 1. The electron density decreases at the surface under the gate and becomes more 'spread out' across the drain region with an increase in work function, indicating a reduction in gate control over the surface. At a work function of 4.75 eV, a high concentration of ionized donors is observed across the drain region, which shows the dopant concentration which has not been utilized for mobile carrier generation, resulting in a lower electron density, which is intuitively understood. The ionized donor concentration and electron density follows the charge neutrality equation of the semiconductor:

$$qp + qN_D^+ - qn - qN_A^- = Q_k \tag{3}$$

where p, n, N_D^+ and N_A^- are the concentration of holes, electrons, ionized donors, and ionized acceptors, respectively, and Q_k is the total charge in the spatial coordinates, which should be maintained constant for specific bias conditions to sustain a constant current. In the drain region, N_A^- is nonexistent and p is negligible. The equation can be rewritten as $qN_D^+ - qn = Q_k$. Therefore, an increase in any one of the variables, be it the ionized donor concentration or the electron density, results in a reduction of the other variables. The contour taken from the TCAD simulations support the trend.

Additionally, the concentration of ionized donors under the influence of the gate-to-source voltage is given in Eq. 1, whereE_D is the donor level,$g_D = 2$ is degeneracy factor for donors, and N_{D0} is the dopant concentration. Equation 1 is dependent on the Fermi level, while the other parameters can be assumed to be constant.

When $E_{FN} - E_D < 0$ and is several kT higher, indicating that E_{FN} lies below E_D by several kT, Eq. 1 sees a decaying exponential term in the denominator for the donor case, resulting in a case of complete ionization. An opposite consideration will result in a case of incomplete ionization where the degree of ionization will be dependent on the relative position of E_{FN} and E_D. This shows that the ionization degree is variable across a semiconductor region and is not constant throughout the region.

For a work function of 4.25 eV at $V_{GS} = 1V$, spatial cutlines were taken at the bottom surface of the silicon body (Fig. 6b) where the ionized donor concentration is highest, and at the top surface of the silicon body (Fig. 6a) where the ionized donor concentration is moderate to minimum. The term $E_{FN} - E_D$ can be written as $(E_C - E_D) - (E_C - E_{FN})$. Taking E_C as the reference, the first term for the *As* dopant species, that is, $E_C - E_D$ is equal to 0.053eV, while is the second term dependent on the Fermi level and conduction band.

Through extraction of the energy band diagram at the two positions of the body, the ionized donor concentration is verified. The details and calculations are listed in Table I.

Figure 7 shows the drain current for φ_M of 4.05eV and 4.75eV in the presence and absence of incomplete ionization. For $\varphi_M = 4.05$eV, we observe considerable deviation of the drain current from $V_{GS} = 0.4$V onward. There is no significant change in the drain current for the φ_M of 4.75eV.

The BTBT rates in the ON state for the different doping-dependent mobility models are depicted in Fig. 8a, where it can be seen that, due to the lack of available carriers, the BTBT rates are reduced in the presence of the incomplete ionization models. In Fig. 8b, the current sensitivity is investigated for different doping-dependent mobility models. The positive V_{GS} range offers a minute sensitivity variation compared to the ambipolar region. There is a higher sensitivity

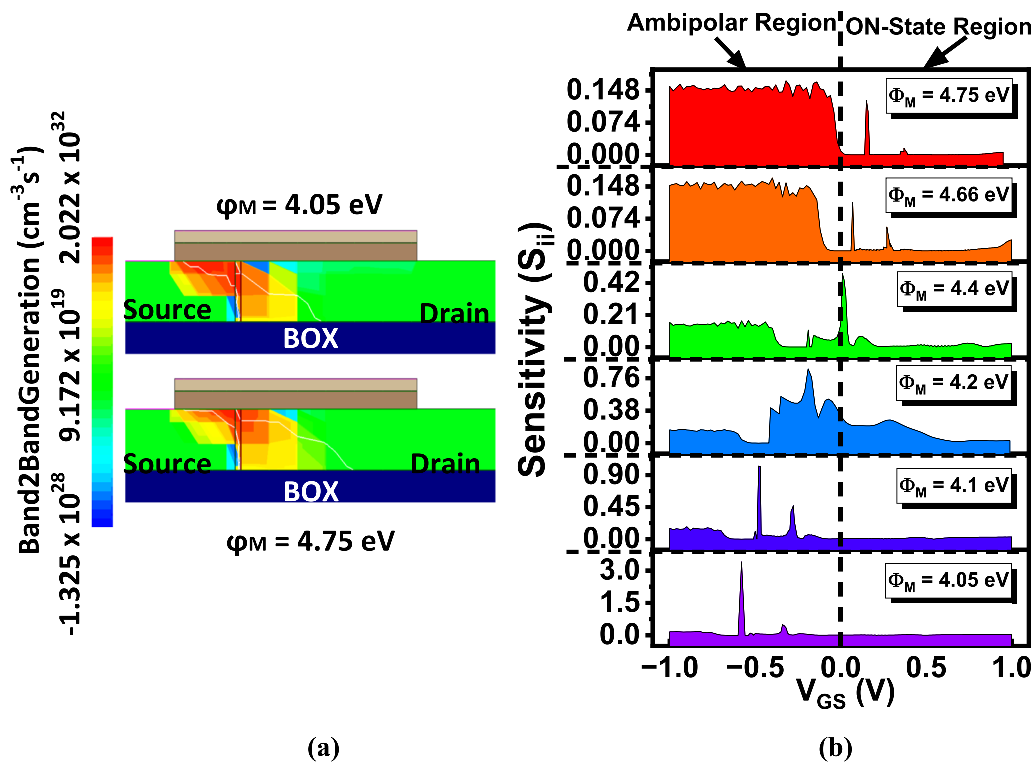

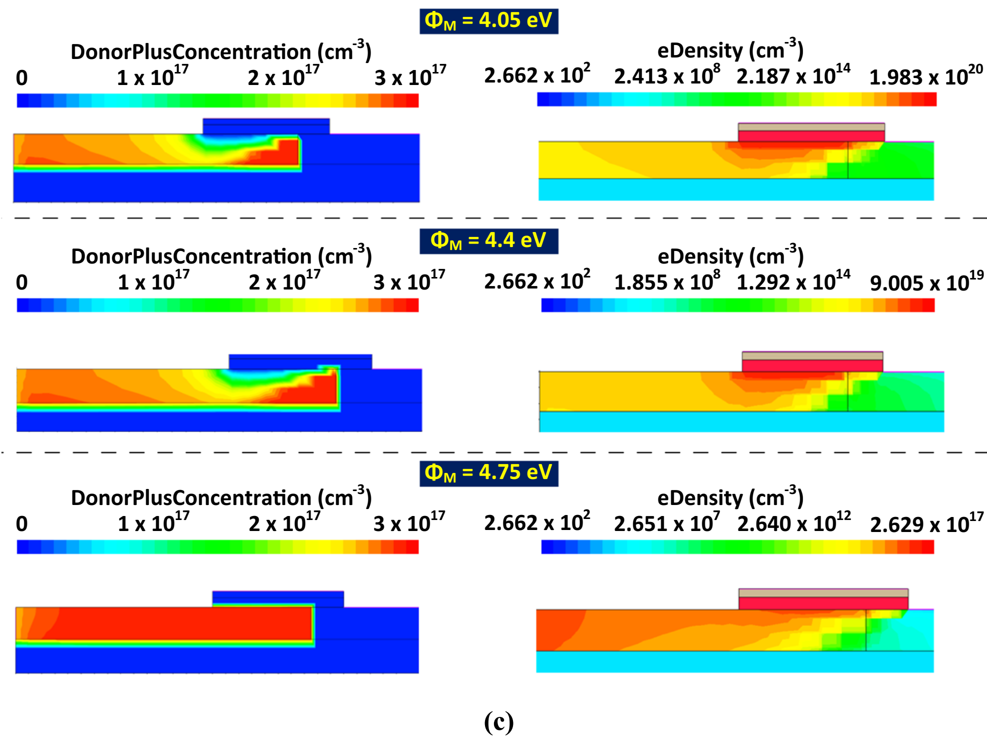

Fig. 5 (a) BTBT contour of the work function φ_M of 4.05eV and 4.75eV; (b) current sensitivity variation for different work functions; (c) contours for both donor plus concentration and electron density for different work functions.

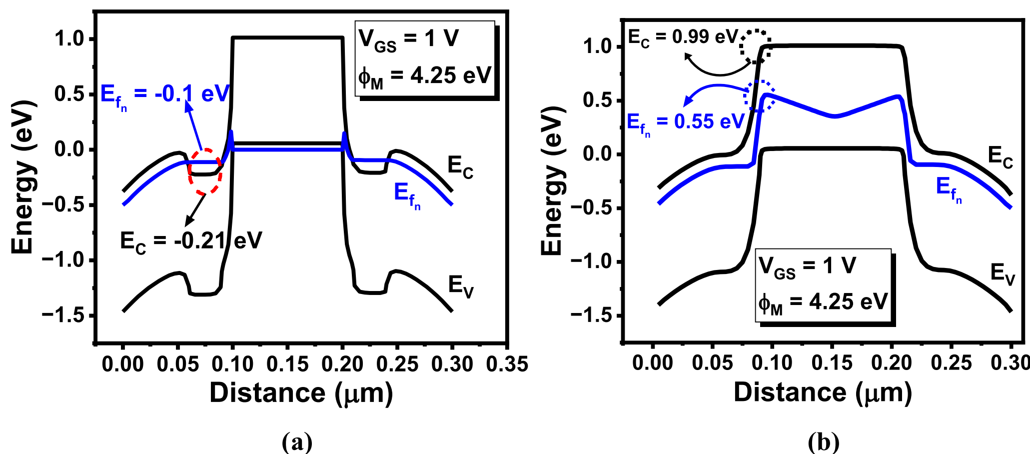

Fig. 6 Energy bands at the spatial cut-line in the (a) oxide/semiconductor interface and (b) bottom surface of the silicon body.

Table I Calculation of ionized donor concentration at two different cut-line positions of the proposed device, showing dependence on $E_{FN} - E_D$

Position of cut-line	Calculation	Ionized donor concentration
At bottom	$N_D = \frac{N_{D0}}{1+g_D.\exp\left(\frac{E_{FN}-E_D}{kT}\right)}$ $N_D = \frac{3\times10^{17}}{1+2.\exp\left(\frac{-0.387}{0.026}\right)}$ $N_D = \frac{3\times10^{17}}{1.000000687}$ $N_{D0} = 2.99\times10^{17}cm^{-3}$ $E_{FN} - E_D = (E_C - E_D) - (E_C - E_{FN})$ $= 0.053eV(forAs) - 0.44eV$ $= -0.387$ $g_D = 2forAs$ $kT = 0.026eV$	$2.99\times10^{17}cm^{-3}$ $N_D \approx N_{D0}$
At surface	$N_D = \frac{N_{D0}}{1+g_D.\exp\left(\frac{E_{FN}-E_D}{kT}\right)}$ $N_D = \frac{3\times10^{17}}{1+2.\exp\left(\frac{0.163}{0.026}\right)}$ $N_D = \frac{3\times10^{17}}{1.056\times10^{3}}$ $N_{D0} = 3\times10^{17}cm^{-3}$ $E_{FN} - E_D = (E_C - E_D) - (E_C - E_{FN})$ $= 0.053eV(forAs) + 0.11eV$ $= 0.163$ $g_D = 2forAs$ $kT = 0.026eV$	$2.84\times10^{14}cm^{-3}$

variation in the ambipolar region in the case of all the models. Towards a further negative range of V_{GS} from −0.5V, the sensitivity gradually increases, reaches the highest sensitivity value, and remains constant for higher ambipolar V_{GS}. A detailed comparison of the mobility models for the proposed device is given in Table II in the Appendix. The

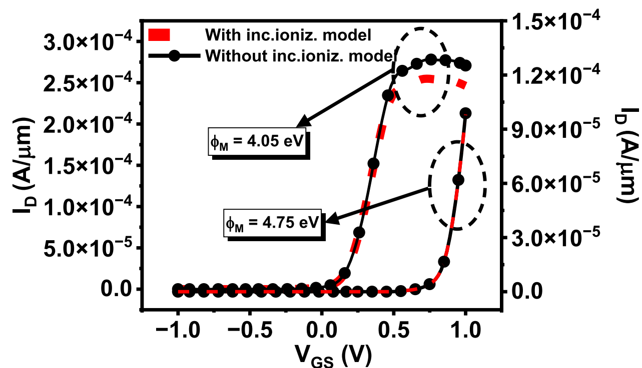

Fig. 7 Transfer characteristics for the proposed device with and without the incomplete ionization model for φ_M = 4.05eV and 4.75eV.

trend in sensitivity and associated important observations are reported here.

The Arora mobility model shows the highest sensitivity spike compared to all the other mobility models, including Masetti, and Philips Unified mobility models. The highest sensitivity spike is present around V_{GS} of −0.19V and tapers down around −0.26V. In the case of Masetti mobility model, there are three distinct sensitivity spikes: the highest one is observed at a V_{GS} of around −0.40V, followed by an adjacent one at V_{GS} of around −0.37V and another one at a V_{GS} of around −0.19V . The Philips Unified mobility model sensitivity variation is similar to the Masetti mobility model except that the former possesses two sensitivity peaks around −0.38V and −0.19V. Overall, a common peak is observed at a V_{GS} of around −0.19V for all the doping-dependent models. The sensitivity plot for the Arora model is observed to be different from the other two doping-dependent models because of its empirical nature (see the Appendix). In the regime of the positive V_{GS} region, humps

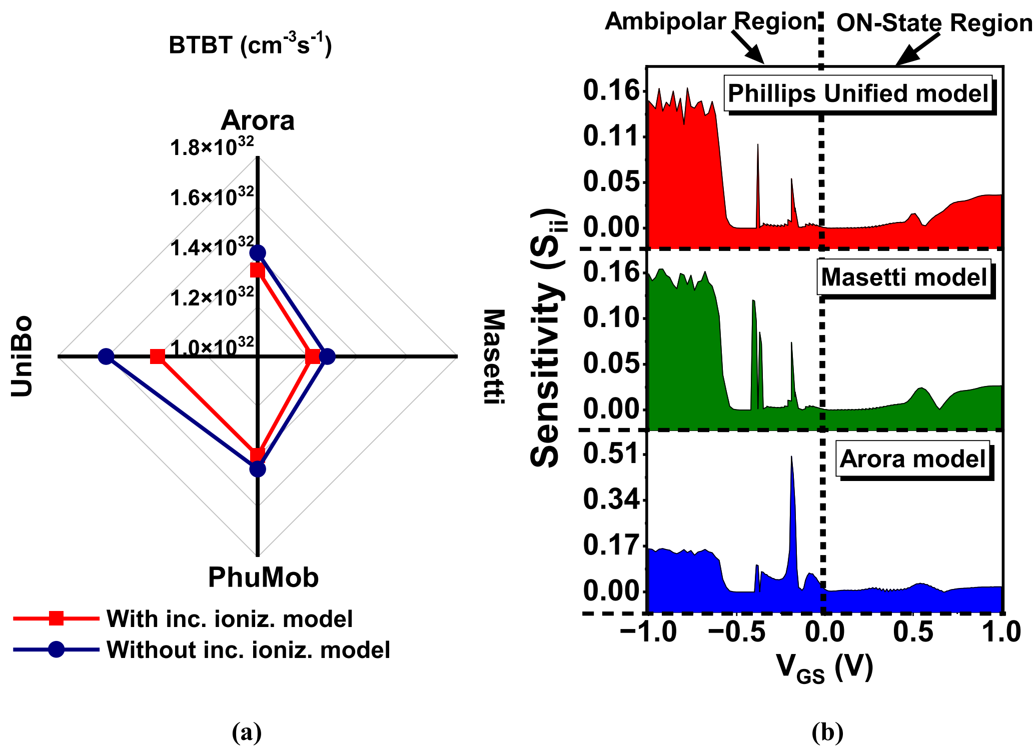

Fig. 8. (a) BTBT for different mobility models; (b) current sensitivity variation for different mobility models.

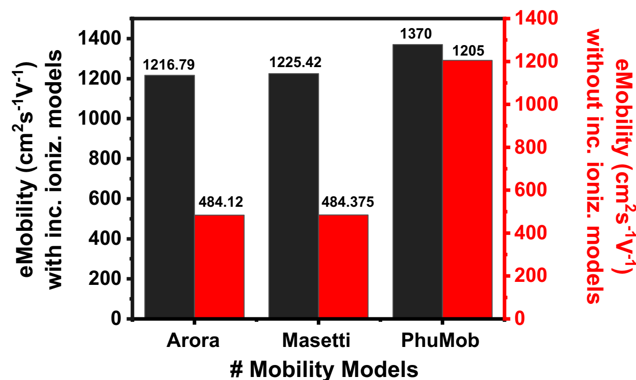

Fig. 9 Comparison of maximum electron mobility of different mobility models in the ON state.

in sensitivity are observed around 0.51 V, 0.55 V, and 0.55 V for the Philips Unified model, the Masetti model, and the Arora model, respectively.

In Fig. 9, we observe maximum electron mobility variation in the TFET in the ON state for different mobility models in the presence and absence of incomplete ionization. We observe considerably higher maximum mobility variation for the simulation carried out with the use of the incomplete ionization model compared to not using the incomplete ionization model during simulation.

Figure 10a shows the BTBT rates for the different mobility degradation models in the presence and absence of incomplete ionization. Unlike the doping-dependent mobility models, the BTBT rates in the mobility degradation models are closer in values when compared between the cases for the presence and absence of incomplete ionization.

In Fig. 10b, the current sensitivity variation is reported for different mobility degradation (E-normal) mobility models. A detailed comparison of the mobility models for the proposed device is given in Table II in the Appendix. The trend in sensitivity and associated important observations are reported here.

The IAL mobility model consists of contributions from the inversion and accumulation layers, and, therefore, it shows a fluctuating sensitivity plot. In the case of the IAL mobility model, the highest sensitivity peak is observed around $V_{GS} = -0.37$V and the second highest peak lies around $V_{GS} = -0.20$V. Like doping-dependent mobility models, there is gradual increase in sensitivity for V_{GS} around −0.5V and the sensitivity becomes constant for more negative V_{GS}. There is very little prominent change in the sensitivity for the positive gate source voltage. The IAL

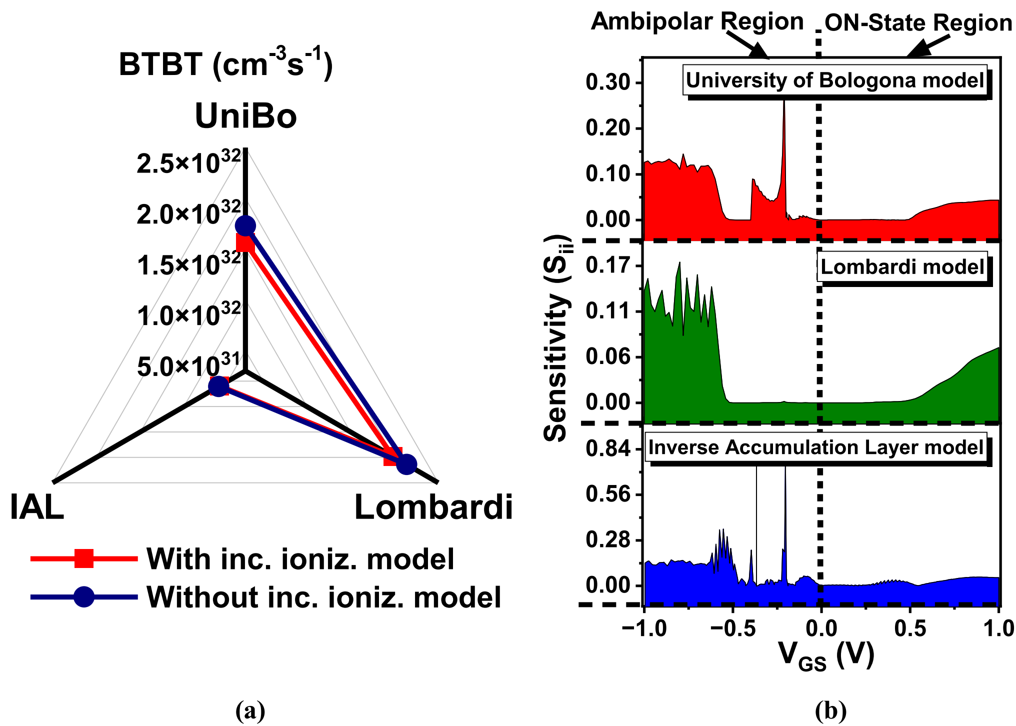

Fig. 10. (a) BTBT for different E-normal mobility models; (b) Current sensitivity variation for different E-normal (degradation) mobility models.

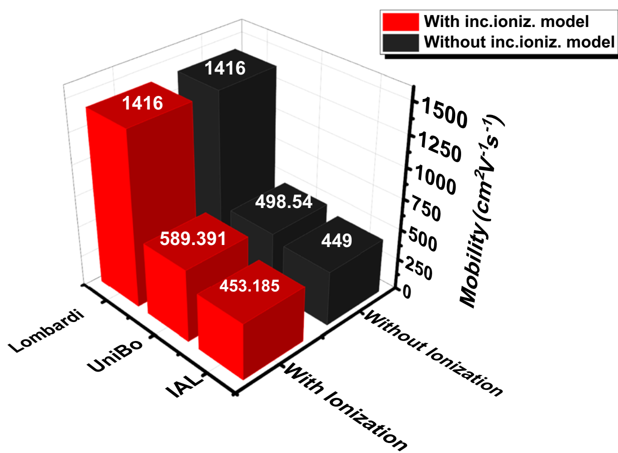

Fig. 11 Maximum e-mobility variation for different E-normal mobility models.

mobility model has the highest sensitivity peaks compared to any other E-normal mobility model.

There is a higher variation in sensitivity across the ambipolar region starting from $V_{GS} = -0.5$V with the highest sensitivity spike around $V_{GS} = -0.21$V in the University of Bologna mobility model. The voltage range between −0.5V and 0.5V shows no change in sensitivity variation in the Lombardi mobility model. The peaks in the University of

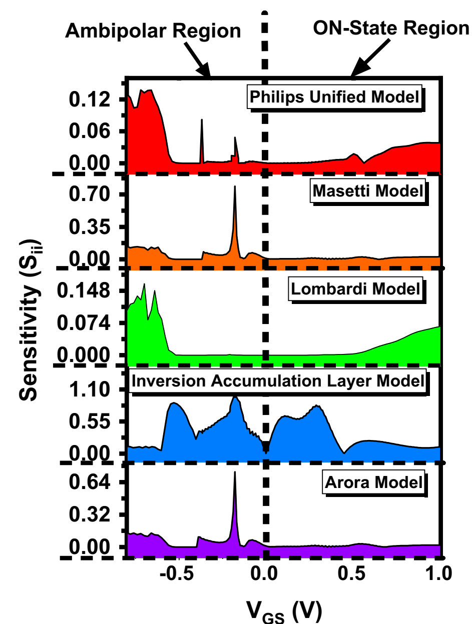

Fig. 12 Plot of sensitivity versus V_{GS} considering trap-assisted tunneling models.

Bologna mobility model and the IAL mobility model can be attributed to Coulomb scattering, as it is a contributing mobility component which is absent in the Lombardi mobility model (see Appendix).

In Fig. 11, we observe the maximum e-mobility variation of the different E-normal mobility models compared for the with and without incomplete ionization models used in the simulator. We come up with an interesting result as there is no significant change in the highest e-mobility values for the with and without incomplete ionization models implemented in the simulator. This can be understood as incomplete ionization not being present or being very minimal in the case of the depletion region under the gate of a MOSFET, which can also be extended for TFETs.[23] Since E-normal mobility models are associated with the interface of the gate oxide layer, we observe no significant change in e-mobility.

The impact of trap-assisted tunneling (TAT) considering the Hurkx model along with trap-assisted Auger recombination on the sensitivity have been considered, where an acceptor-like Gaussian trap density of states have been considered at the oxide/semiconductor interface.[24] A peak concentration of 10^{13}cm^{-3} and a peak energy trap level of 0.55 eV from the valence band edge have been taken for the trap-assisted models. Another observation can be made from this analysis, because, as the gate voltage increases, the sensitivity curve for the different mobility models becomes saturated. There is a large similarity in the trends in sensitivity for the doping-dependent mobility models (Masetti, Arora, and Philips Unified) with and without the TAT model. The presence of TAT reduces the area of high sensitivity in the ambipolar region (negative V_{GS}). The common peaks of sensitivity for the three models are observed at V_{GS} close to −0.19V, indicating that the effect of TAT on the sensitivity is similar in terms of the location of the peak. A similar trend is also observed for the E-normal (mobility degradation models), except for the IAL mobility model, because it considers the scattering associated with the inversion layer. Due to the presence of trap states in the interface, the carrier population across the inversion (or accumulation) layer will be highly influenced (see Appendix) (Fig. 12).

Conclusions

This work reports the influence of incomplete ionization on current sensitivity due to different gate work functions, doping-dependent mobility models, and mobility degradation models. The significant conclusions of the work are:

- Current sensitivity peaks shift towards the positive V_{GS} axis and decrease in magnitude with the increase in the gate work function.
- The ionized donors and the electrons maintain a charge neutrality at a particular bias which can be observed from the ionized donor concentration profile and electron density profile.
- Among the doping-dependent mobility models, there is a qualitative relationship between the magnitude of the sensitivity spikes and the sensitivity in the negative V_{GS} regime. The magnitude of the spikes decreases as compared to the magnitude of the sensitivity in the negative V_{GS} regime in the order Arora, Masetti, and Philips Unified mobility models.
- Among the three mobility degradation models considered in this work, the IAL mobility model shows high sensitivity spikes, followed by the University of Bologna model. The Lombardi model does not exhibit spikes and the profile stays flat for the intermediate V_{GS} regime.
- In the presence of the trap-assisted tunneling model (TAT), the IAL mobility model shows a greater change in its trend of sensitivity compared to its case without TAT because it is related to the inversion and accumulation layers of the device, which are greatly influenced by the interface traps.

Appendix

A comparison is listed among all the models in the form of a table along with analytical expressions and dependencies. The mobility contour of the device for both cases of incomplete and complete ionization has been provided.

See (Table II).

Table II Comparison of incomplete-ionization-dependent mobilities in double gate n-p-n TFETs

Mobility model	Expression and explanation	Electron Mobility Contours (incomplete ionization: *top*; complete ionization: *bottom*)
Masetti[15] (*Doping dependent mobility*)	$\mu = \mu_0 e^{-\gamma} + \frac{\mu_{max} - \mu_x}{1 + (\frac{x}{C_r})^{\alpha}} - \frac{\mu_1}{1 + (\frac{C_s}{x})^{\beta}}$ [15] Parameters — As — B γ — 0 — $\frac{-P_C}{P}$ x — n — P μ_x — μ0 — 0 The effect of ionized donor and acceptor concentration is taken into consideration for this mobility model where n and p are ionized donor and acceptor concentration respectively. The first two terms give us an inverse relationship with respect to ionized donor and acceptor concentration. The third term of the equation becomes relevant for high doping concentration taking into account further dip in mobility for high doping concentration.	We observe a constant mobility value across the drain region for the lower diagram. This is due to the fact that the dopants are completely ionized across the drain region since incomplete ionization model is not activated for this case. For the top contour incomplete ionization model is activated for this case. We observe an enhanced mobility value across the drain region for this case due to the fact that lesser number of ionized impurities are present for incomplete ionization case leading to higher mobility due to inverse relationship of mobility with ionized donor or acceptor concentration.

Table II (continued)

Mobility model	Expression and explanation	Electron Mobility Contours (incomplete ionization: *top*; complete ionization: *bottom*)
Arora (*Doping dependent mobility*)	$\mu = xT_n^{-0.57} + \frac{yT^{-2.33}}{1+[\frac{N}{(zT_n^{2.4})^{0.88T_n^{-0.146}}}]}$ where T_n=T/300[15] Parameters — As — B x — 88 — 54 y — $7.4X10^8$ — $1.36X10^8$ z — $1.26X10^{17}$ — $2.35X10^{17}$ This model takes into consideration the effect of temperature and comes up with an empirical relationship for both electrons and holes. We observe an inverse relationship of mobility with respect to ionized donor or acceptor concentration denoted by N. The phenomenon that has been taken into consideration for modelling includes integrated effects of lattice and ionized impurity scattering.	We observe higher mobility values for the top contour which takes into consideration the incomplete ionization model reducing ionized donor concentration hence resulting in enhanced mobility values. The lower contour considers the donor concentration across the drain region to be completely ionized increasing its concentration hence resulting in lower mobility values. We observe very minute decrease of mobility compared to Masetti model for this case as for higher doping concentration this model takes into consideration both electron-electron and hole-hole scattering. However, there is a little compensation in mobility reduction due to consideration of anisotropic scattering (forward scattering) leading to very similar mobility values for both the doping dependent models. We observe very high mobility below the interface of the oxide region. This is due to the fact that there is presence of very high electron density across the region. This leads to reduction in ionized donor concentration which is validated by charge neutrality equation [Eq. (3)]. The reduction in ionized donor concentration leads to enhancement of mobility across that region.

Table II (continued)

Mobility model	Expression and explanation	Electron Mobility Contours (incomplete ionization: *top*; complete ionization: *bottom*)
Philips Unified[15] (*Doping dependent mobility*)	This mobility model takes into consideration predominantly four mobility degradation factors which can be combined together using the Matthiesen rule given below.	
	$\mu_i^{-1} = \mu_{i,L}^{-1} + \mu_{i,D}^{-1} + \mu_{i,A}^{-1} + \mu_{i,j}^{-1}$[15] here, j are holes if i is electron or j are electrons if i is hole while N_A and N_D are ionized acceptor and donor concentration. $\mu_{i,L}$ is mobility scattering factor associated with the lattice which is dominant at very low doping. $\mu_{i,D}$ takes into consideration majority carrier scattering which also takes into consideration the effect of carrier screening. The third term of the equation describes the mobility of minority impurity scattering associated with both holes or electrons for donors and acceptors respectively. The fourth term of the equation takes into account the effect of electron hole scattering which is attractive in nature. In this model the electrons are regarded as moving acceptors while holes are regarded as moving donors.	We observe the highest electron mobility across the interface of oxide compared to two other doping dependent mobility models. This is due to the fact that the effect of screening of carriers is taken into consideration of this mobility model. This leads to reduction of mobility as we move away from the interface region.

Table II (continued)

Mobility model	Expression and explanation	Electron Mobility Contours (incomplete ionization: *top*; complete ionization: *bottom*)
Lombardi[15] (*Interface mobility degradation model*)	$\frac{1}{\mu}=\frac{1}{\mu_b}+\frac{D}{\mu_{ac}}+\frac{D}{\mu_{sr}}$ [15]	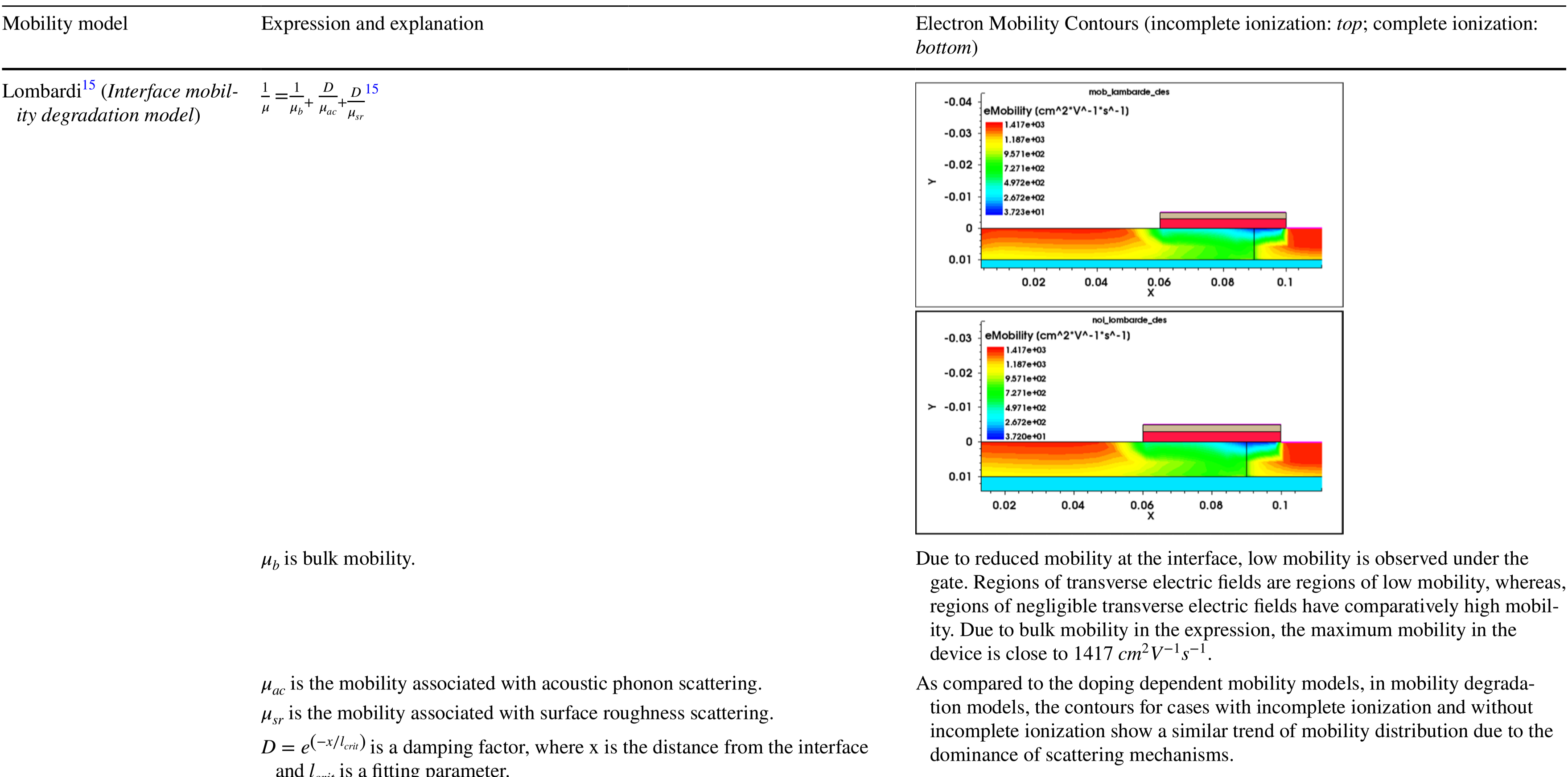
	μ_b is bulk mobility.	Due to reduced mobility at the interface, low mobility is observed under the gate. Regions of transverse electric fields are regions of low mobility, whereas, regions of negligible transverse electric fields have comparatively high mobility. Due to bulk mobility in the expression, the maximum mobility in the device is close to 1417 $cm^2V^{-1}s^{-1}$.
	μ_{ac} is the mobility associated with acoustic phonon scattering. μ_{sr} is the mobility associated with surface roughness scattering. $D = e^{(-x/l_{crit})}$ is a damping factor, where x is the distance from the interface and l_{crit} is a fitting parameter.	As compared to the doping dependent mobility models, in mobility degradation models, the contours for cases with incomplete ionization and without incomplete ionization show a similar trend of mobility distribution due to the dominance of scattering mechanisms.

Table II (continued)

Mobility model	Expression and explanation	Electron Mobility Contours (incomplete ionization: *top*; complete ionization: *bottom*)
University of Bologona[15] (*Interface mobility degradation model*)	$\frac{1}{\mu}=\frac{1}{\mu_{bsc}}+\frac{D}{\mu_{ac}}+\frac{D}{\mu_{sr}}$ [15]	
	μ_{bsc} is mobility associated with Coulomb scattering.	Compared to Lombardi model, the maximum electron mobility in the device is reduced to lower than half of bulk mobility due to the addition of contribution from Coulomb scattering. The screening is due to contribution from impurities and carrier concentration. Since the bulk mobility is absent in the expression, the model has stronger interface-specific phonon and surface roughness scattering as evident from the damping factor, D in the two terms.
	μ_{ac} is the mobility associated with surface acoustic phonon scattering. μ_{sr} is the mobility associated with surface roughness scattering. $D = e^{(-x/l_{crit})}$ is a damping factor, where x is the distance from the interface and l_{crit} is a fitting parameter.	At high transverse fields, the phonon and surface roughness scattering mechanisms are dominant due to their inverse relationship with the electric field. Reduced mobility under the gate is observed similar to the Lombardi model; however, there is a *beak* shape of high mobility in the drain close to the region away from the interface along lateral direction, which can be attributed to Coulomb scattering.

Table II (continued)

Mobility model	Expression and explanation	Electron Mobility Contours (incomplete ionization: *top*; complete ionization: *bottom*)
Inversion Accumulation Layer[15] (*Interface mobility degradation model*)	$\frac{1}{\mu}=\frac{1}{\mu_c}+\frac{1}{\mu_{ph}}+\frac{D}{\mu_{sr}}$ [15]	
	where, μ_c is the mobility associated with Coulomb scattering, μ_{ph} is the mobility associated with phonon scattering and μ_{sr} is the mobility associated with surface roughness scattering. $D = e^{(-x/l_{crit})}$ is a damping factor, where x is the distance from the interface and l_{crit} is a fitting parameter.	The distribution of mobility for IAL mobility model is similar to the University of Bologna model, except that the *beak* shape of high mobility is reduced. The Coulomb scattering has contributions from the inversion and accumulation layer of the region along with dependence on local layer thickness. The nature of this difference from the University of Bologna model makes the distribution slightly different in this case.

Acknowledgment This work is partly supported by DST-FIST II, vide sanction no. SR/FST/ET-II/2018/241.

Conflict of interest The authors declare that they have no conflict of interest.

References

1. S. Poria, S. Garg, and S. Saurabh, in *Suppression of Ambipolar current in Tunnel Field-Effect Transistor using Field-Plate*. 2020 24th International Symposium on VLSI Design and Test (VDAT), 1–6 (2020)
2. G.L. Priya and N.B. Balamurugan, New dual material double gate junctionless tunnel FET: subthreshold modeling and simulation. *AEU-Int. J. Electron. C.* 99, 130–138 (2019).
3. U.E. Avci, D.H. Morris, and I.A. Young, Tunnel field-effect transistors: prospects and challenges. *IEEE J. Electron Devices Soc.* 3, 88–95 (2015).
4. M. Aswathy, N.M. Biju, and R. Komaragiri, in *Simulation studies of tunnel field effect transistor (TFET)*. 2012 International Conference on Advances in Computing and Communications, 138–141 (2012)
5. S.O. Koswatta, M.S. Lundstrom, and D.E. Nikonov, Performance comparison between pin tunneling transistors and conventional MOSFETs. *IEEE Trans. Electron Devices* 56, 456 (2009).
6. D.B. Abdi and M.J. Kumar, Controlling ambipolar current in tunneling FETs using overlapping gate-on-drain. *IEEE J. Electron Devices Soc.* 2, 187 (2014).
7. P.P. Altermatt, A. Schenk, B. Schmithüsen, and G. Heiser, A simulation model for the density of states and for incomplete ionization in crystalline silicon. II. Investigation of Si: As and Si: B and usage in device simulation. *J. Appl. Phys.* 100(11), 113715 (2006).
8. M. Forster, F.E. Rougieux, A. Cuevas, B. Dehestru, A. Thomas, E. Fourmond, and M. Lemiti, in *Incomplete ionization and carrier mobility in compensated p-type and n-type silicon*. 2012 IEEE 38th Photovoltaic Specialists Conference (PVSC) PART 2, Austin, TX, USA, 1–6 (2012)
9. P.P. Altermatt, A. Schenk, and G. Heiser, A simulation model for the density of states and for incomplete ionization in crystalline silicon. II. Establishing the model in Si:P. *J. Appl. Phys.* 100(11), 113714 (2006).
10. A. Akturk, M. Peckerar, M. Dornajafi, N. Goldsman, K. Eng, T. Gurrieri, and M.S. Carroll, in *Impact ionization and freeze-out model for simulation of low gate bias kink effect in SOI-MOSFETs operating at liquid he temperature*. 2009 International Conference on Simulation of Semiconductor Processes and Devices, 1–4 (2009)
11. D.C. Colea and J.B. Johnson, in *Accounting for incomplete ionization in modeling silicon based semiconductor devices*. Proceedings of the Workshop on Low Temperature Semiconductor Electronics, 73–77 (1989)
12. N. Donato and F. Udrea, Static and dynamic effects of the incomplete ionization in superjunction devices. *IEEE Trans. Electron Devices* 65, 4469 (2018).
13. W.Y. Choi, B.G. Park, J.D. Lee, and T.J.K. Liu, Tunneling field-effect transistors (TFETs) with subthreshold swing (SS) less than 60 mV/dec. *IEEE Electron Device Lett.* 28, 743 (2007).
14. D. Deb, R. Goswami, R.K. Baruah, K. Kandpal, and R. Saha, Parametric investigation and trap sensitivity of npn double gate TFETs. *Comput. Electr. Eng.* 100, 107930 (2022).
15. TCAD, Sentaurus device user's manual. Mountain View: CA:USA: TCAD; (2022)
16. G. Masetti, M. Severi, and S. Solmi, Modeling of carrier mobility against carrier concentration in arsenic-, phosphorus-, and boron-doped silicon. *IEEE Trans. Electron Devices* 30(7), 764 (1983).
17. N.D. Arora, J.R. Hauser, and D.J. Roulston, Electron and hole mobilities in silicon as a function of concentration and temperature. *IEEE Trans. Electron Devices* 29(2), 292 (1982).
18. D.B.M. Klaassen, A Unified mobility model for device simulation—I. Model equations and concentration dependence. *Solid-State Electron.* 35(7), 953 (1992).
19. S. Reggiani, M. Valdinoci, L. Colalongo, and G. Baccarani, in *A Unified analytical model for bulk and surface mobility in Si n-and p-channel MOSFET's*. 29th European Solid-State Device Research Conference, vol. 1, 240–243 (1999)
20. C. Lombardi, S. Manzini, A. Saporito, and M. Vanzi, A physically based mobility model for numerical simulation of nonplanar devices. *IEEE Trans. Comput. Aided Des. Integr. Circuits Syst.* 7, 1164 (1988).
21. S.A. Mujtaba, Advanced mobility models for design and simulation of deep submicrometer MOSFETs. Stanford University (1995)
22. A.M. Ionescu and H. Riel, Tunnel field-effect transistors as energy-efficient electronic switches. *Nature* 479(7373), 329 (2011).
23. A. Schenk, P.P. Altermatt, and B. Schmithusen, in *Physical model of incomplete ionization for silicon device simulation*. 2006 International Conference on Simulation of Semiconductor Processes and Devices, 51–54 (2006)
24. D. Deb, R. Goswami, R.K. Baruah, R. Saha, and K. Kandpal, Role of gate electrode in influencing interface trap sensitivity in SOI tunnel FETs. *J. Micromech. Microeng.* 32, 044006 (2022).

Publisher's Note Springer Nature remains neutral with regard to jurisdictional claims in published maps and institutional affiliations.

Springer Nature or its licensor (e.g. a society or other partner) holds exclusive rights to this article under a publishing agreement with the author(s) or other rightsholder(s); author self-archiving of the accepted manuscript version of this article is solely governed by the terms of such publishing agreement and applicable law.